Environmental Science
Water Research & Technology

Electrochemical degradation of perfluoroalkyl acids by titanium suboxide anodes

Journal:	*Environmental Science: Water Research & Technology*
Manuscript ID	EW-ART-08-2019-000759.R3
Article Type:	Paper

Electrochemical degradation of perfluoroalkyl acids by titanium suboxide anodes

Yaye Wang[a, †], Randall "David" Pierce, Jr.[a, †], Huanhuan Shi[a,b], Chenguang Li[a,b], Qingguo Huang[a,*]

[a] College of Agricultural and Environmental Sciences, Department of Crop and Soil Sciences, University of Georgia, Griffin, GA 30223, United States.

[b] State Key Laboratory of Pollution Control and Resources Reuses, School of the Environment, Nanjing University, Nanjing 210023, P. R. China

[†] These authors contributed equally to this study.

[*] Corresponding author, E-mail: qhuang@uga.edu.

Abstract

Our recent findings indicate effective electrochemical degradation of perfluoroalkyl acids (PFAAs) in aqueous solutions using novel titanium suboxide (TSO) anodes. This provides a potentially promising technology to treat per- and polyfluoroalkyl substances (PFAS) in legacy AFFF stockpiles or in wastewater and contaminated groundwater. The degradation of PFAAs in TSO-based electrooxidation was evaluated with solutions of different compositions containing eight PFAAs either individually or in mixture and under a range of operation conditions. Surface area normalized pseudo-first order rate constants were obtained and interpreted in terms of PFAA degradation behaviors and mechanisms. The PFAA degradation rates were further correlated to the molecular and electronic descriptors of the chemicals calculated based on density functional theory. The results of the study further the understanding of PFAS degradation in TSO-based anodic oxidation, and provide a basis for process optimization, design and scaling.

Water Impact- With the development of PFAS as a major water contaminant concern, treatment technologies have become needed for these highly stable compounds. Our work herein presents a promising treatment method by electrooxidation using titanium suboxide anode for the degradation of multiple PFAS species.

1. Introduction

Per- and polyfluoroalkyl substances (PFAS) have been used in industrial applications since the latter half of the 20th century primarily as surfactants suited for harsh conditions because of their extreme chemical and thermal stability. These compounds obtain their high stability largely due to C-F bonds that replace the typical C-H bond in organic molecules [1]. PFAS have emerged as a public concern because of their persistence in the environment, bioaccumulation tendency and risks to human and other biological populations [2]. In particular, perfluoroalkyl acids (PFAAs) pose a unique threat as degradation of many PFAS become persistent PFAA byproducts during many technological and biological degradation processes [3 4]. PFAAs comprise some of the most well-known PFAS such as perfluorooctanesulfonate (PFOS) and perfluorooctanoic acid (PFOA).

Wildlife and human monitoring services have identified PFAAs in mammal populations spanning the entire planet with PFAAs levels in human plasma having been reported over the past two decades[5 6 7 8].

Trends appear to be correlated with geographic and temporal exposure. Although the correlation of industrial output and biological levels of these contaminants is likely, the fate and persistence in environments lacks definitive research, including the mechanisms behind biological uptake [8]. Toxicological research into the reported quantities of PFAS in mammals is also still in its infancy, but studies suggest they are particularly related to developmental toxicity, immunotoxicity, and hepatotoxicity [5].

As the toxicological impacts of PFAS have become evident, treatment methods for PFAS polluted ground and waste waters have been explored. Unfortunately both traditional wastewater remediation techniques and even many advanced oxidation processes (AOPs) have not been successful in PFAA treatment due to their extreme chemical stability [9]. Development of certain techniques have reported some success at treating PFAAs such as photochemical decomposition [10 11 12], ultrasonic irradiation[13], and heat induced persulfate oxidation [14], but the application of these technologies is limited because of their high energy input and harsh operating conditions.

Recent research into electrochemical oxidation has emerged at the forefront of PFAS treatment because of its robustness and ability to use under benign conditions. Electrochemical degradation of PFAAs has been successful in recent studies using boron doped diamond (BDD) and Sb and Pb doped titanium based anodes under ambient conditions for spiked samples [15 16 17 18] and BDD has demonstrated success using real world waste water effluents [19]. While efficient degradation and mineralization has been achieved in some studies, drawbacks exist[20]. These drawbacks regarding the high cost of BDD based anodes, generation of disinfection byproduct and potential toxic by-products release by Sb and Pb doping agents have been a major limitation in the implementation of these technologies[16].

We have recently investigated the use of Magnéli phase titanium suboxide (TSO) anodes for PFAS degradation because of their potential low cost of commercial production, high conductivity, and robustness [21]. These materials consist of a series of sub-stoichiometric titanium oxides with the formula of Ti_nO_{2n-1} where n is an integer between 3 and 10; Ti_4O_7 is the most desired variant because it has the highest electrical conductivity[21]. Recent studies have shown the viability of Ti_4O_7 based anodes for electrochemical remediation of aqueous organic pollutant such as phenols and tetracycline [22 23 24]. Early work done on the remediation of PFOA and PFOS using the TSO anodes yielded promising results [25 26, 27], removing more than 95% of PFOA and PFOS in a batch system at 10 $mA \cdot cm^{-2}$ after 3 hours[25] and more than 99% of PFOA and PFOS in a reactive electrochemical membrane (REM) system at the anodic potential of 2.9 V vs. SHE with a constant permeate flux of 36 LMH[27]. However, the impact of different compositions of PFAS is still unknown, both in terms of their respective degradation rates and possible competition behaviors, and requires further exploration [25]. Knowledge on the behavior of PFAS mixture is much needed, because multiple PFAS are often used and present together [3]. This study assessed eight PFAAs (PFBA, PFPeA, PFHxA, PFHpA, PFOA, PFBS, PFHxS and PFOS), either individually or in mixture, by TSO-based electrooxidation across a range of anodic potentials in solutions of different compositions. The treatment performance was explored in terms of key operation conditions as well as the molecular features of the chemicals.

2. Experimental Section

2.1 Chemicals and Standards

Mass-labelled perfluoro-n-[$^{13}C_8$] octanoic acid (M8PFOA) and sodium perfluoro-n-[$^{13}C_8$] octanesulfonate (M8PFOS) were obtained from Wellington Laboratories Inc (Guelph, Ontario, Canada,). Perfluorooctanoic acid (PFOA, >97%) and Perfluorohexanesulfonic acid (PFHxS, 98 %) were purchased from Sigma Aldrich Chemical Co., Ltd (St. Louis, Missouri). Perfluorobutanoic acid (PFBA, 98%),

perfluorobutanesulfonic acid (PFBS, 97%), perfluopentanoic acid (PFPeA, 97%), and perfluoheptanoic acid (PFHpA, 97%) were also from Sigma Aldrich. Perfluoroctanesulfonic acid (PFOS, 98%) was purchased from Indofine chemical company, Inc. (Hillsborough, NJ). Perfluorohexanoic acid (PFHxA, 98%) was purchased through Tokyo Chemical Industries (Tokyo, Japan). Sodium sulfate (>99.0%), sodium nitrate (>99.1%), and sodium hydroxide (>98%) were purchased from J.T. Baker (Phillipsburg, New Jersey). Monobasic sodium phosphate ($H_2NaPO_4 \cdot 2H_2O$) (99%) was purchased from Alfa Aesar (Ward Hill, Massachusetts). Dibasic sodium phosphate ($Na_2HPO_4 \cdot 7H_2O$) (>98%) was from EM Science (Gardena, CA).

2.2 Electrochemical Oxidation Experiment

The electrochemical oxidation experiments were conducted in a rectangular reactor (10 cm×5 cm×2.5 cm) containing 200 mL target solution, with one TSO plate (10 cm×5 cm) placed in the middle as anode and two stainless steel of the same size on either side in parallel as cathodes. The reactor was made of acrylic materials, and the TSO electrodes were custom-made according to a method used in our previous study[26, 28]. The distance between the electrodes is 2.5 cm (see Figure S1 for a picture). A DC power supply unit (303 DM supplied by Electro Industries Inc) was used to supply electricity at constant current, and the solution was stirred by a magnetic stirrer at a constant speed throughout each experiment. Electric current density was calculated using the submerged surface area on both sides of the anode (total geometric surface area is 78 cm^2). The anodic potential was monitored using a CHI 660E electrochemical workstation (CH Instruments, Inc., Austin, TX) with Ag/AgCl reference electrode placed 0.3 cm from the anode, and all potentials are reported against standard hydrogen electrode (SHE) with internal resistance compensation. The reaction solution was prepared with each PFAA at the initial concentration of 2.0 μM, either individually or in a mixture, with 100 mM Na_2SO_4 as supporting electrolytes, unless otherwise specified. The electric current was applied after 30 minutes of solution stirring in the reactor. Aliquots of samples, 400 μL each, were collected at prescribed time intervals, and the samples were taken after pausing the current for 90 seconds while maintaining stirring to ensure solution homogeneity. pH was also measured during this period by an ion selective electrode (Oakton pH 300 series). A wash procedure was used on electrodes between experiments, including submersion in deionized water while sonicating for one hour, in methanol for one hour, in 0.1M HCL for one hour, and finally in deionized water again for one hour. The PFAA concentration used in this study was greater than those typically present in contaminated groundwater for ease of sample handling and analysis.

2.3 Chemical analysis

Each sample was diluted 1:1 with 0.10 μM M8PFOA and M8PFOS in MeOH and filtered through a nylon-based syringe filter. Samples were processed through a UPLC-MS/MS system (Waters I-class UPLC; Water Xevo TQD triple quadrupole mass spectrometer) in negative electrospray ionization mode using multiple reaction monitoring (MRM). The UPLC was operated with methanol (A) and water (B) (5 mM ammonium acetate in each) as the mobile phases at a flow rate of 0.3 $mL \cdot min^{-1}$ using a gradient condition listed in Table S1. Electrospray ionization (ESI) was operated in a negative mode with capillary voltage at 1.14 kV, cone voltage 60 V, source temperature at 400 °C and desolation temperature at 550 °C. The mass transitions and spectrometry conditions for MRM monitoring are specified in Table S2. Mass labeled PFOS and PFOA were used as internal standards, with M8PFOS for perfluoroalkylsulfonates (PFSAs) and M8PFOA for perfluoroalkyl carboxylic acids (PFCAs). Quantification was achieved by the ratio of the MRM signal of the chemical to that of the internal standard in reference to a five-point calibration curve.

Fluoride ion concentrations were analyzed in selected samples. The analysis was performed using a F^- ion selective electrode (Thermo Scientific™ Orion™) with a reported detection limit of 0.01 ppm by a standard-addition method[29], with detail described in Text S3.

2.4 Electrode Characterization

The characterization of TSO anodes used in this study has been reported in our earlier study [25]. It is primarily composed of Ti_4O_7 as indicated by X-ray diffraction analysis (Figure S2 A and B) and have interconnected micropores (Figure S2 C) with sizes ranging roughly from 0.8 to 9 μm as shown by mercury intrusion analysis (Figure S2 D). Linear sweep voltammetry (LSV) was performed at the scan rate of 100 $mV \cdot s^{-1}$ using a CHI 660E electrochemical workstation (Austin, TX) by a three-electrode setup, with Ti_4O_7 as the working electrode (1 cm × 1 cm), a 304 stainless steel rod (10 cm × 0.3 mm) as the counter electrode, and a single-junction saturated silver chloride electrode (SCE) as the reference electrode (Pine Research Instruments, Grove City, PA, USA).

2.5 Molecular simulation

Quantum mechanical computation was performed using Gaussian 09 based on the density functional theory (DFT) at B3LYP/6-311G** level. The molecular geometry was optimized and vibrational frequencies computed for each PFAA, based on which a suite of molecular descriptors were calculated, including the frontier electron densities (FEDs) of the highest occupied molecular orbital (HOMO) and the lowest unoccupied molecular orbital (LUMO), the energy level of HOMO (E_{HOMO}) and LUMO (E_{LUMO}) and their gap (E_{LUMO}-E_{HOMO}), and molecular polarizabilities.

3. Results and Discussion

3.1 PFAA degradation

Experiments were performed to examine electrooxidation in solutions having each of the eight PFAAs spiked individually using TSO anode at 5 $mA \cdot cm^{-2}$ current density. Figure 1 shows the results for PFOA and PFOS. It is evident that the concentration of PFOA or PFOS decreased rapidly over time upon electrolysis, and the time-course data are well fitted by the pseudo-first order rate equation (Text S1). Both linear and branched PFOS (L-PFOS and B-PFOS) were contained in the PFOS sample tested, and the ratio between them was approximately 16.5 (L-PFOS / B-PFOS) based on their responses in MRM. Both L-PFOS and B-PFOS were monitored separately during the experiment, and the data of each are shown in Figure S3. The degradation behaviors of L-PFOS and B-PFOS are close to each other (Figure S3), and thus only L-PFOS data were reported in the ensuing discussion. Control experiments were performed in the same system with no current applied (Figure S4). The result indicates that adsorption of PFOS and other PFAAs on the TSO anode is minimal.

It is possible that shorter chain PFAAs may be formed from the degradation of longer chain PFAAs. Therefore, when the electrooxidation of PFOA was tested individually, all PFAAs tested in this study were quantified. Results showed minimal potential byproduct formation (<1%) for PFOA (Figure S5), and this result is consistent with our earlier findings[26]. It indicated that the negatively charged substrates may be held on anode and undergo further degradation and mineralization.

The data of all eight PFAAs were fitted to the pseudo-first order rate model to calculate the rate constant and then normalized to the anode effective electroactive surface area (Text S1) to obtain surface area normalized rate constant (k_{SA}). The effective electroactive surface area of the anode is 468.05 cm^2, and the method for calculating effective electroactive surface area was presented in Text S2. Based on a previous work[30], the potential drop in the pores of TSO may have some effect on the EESA, albeit not significant

(Text S2). However, since the pore size is not uniform in the TSO anode used in this study, the potential drop cannot be accurately calculated and thus not addressed in this study.

Table 1 listed the k_{SA} values for all eight PFAAs for comparison. In general, the degradation of longer chain ones appeared to be faster, and those of PFSAs were faster than PFCAs at the experimental conditions. A discussion based on quantitative structure-activity relationship study is presented later in the study. The k_{SA} values obtained in this study for PFOA (5.74×10^{-6} m·s^{-1}) and PFOS (8.81×10^{-6} m·s^{-1}) were comparable to our previous study using a similar batch reactor setup[26], but are significantly lower than a recent study using a reactive electrochemical membrane (REM) reactor that were 4.40×10^{-5} m·s^{-1} for PFOA and 1.30×10^{-4} m·s^{-1} for PFOS[27]. This is not surprising because a REM operation can significantly enhance mass transfer and thus electrochemical reactions on anode surface.

3.2 Effect of pH and Electrolyte

The impact of pH on PFOS degradation during electrooxidation was evaluated with the TSO anode at the current density of 5.0 mA·cm^{-2} in solution of 50-mM H_2SO_4, 100-mM NaOH and 100-mM phosphate buffer, respectively. The surface area normalized rate constant (k_{SA}) of L-PFOS degradation obtained in these solutions are shown in Table 2. The k_{SA} value was slightly smaller in the acidic solution, probably because of the lower anodic potential in this solution than the other two solutions. The influence of the bulk solution pH is expected to be minimal because PFOS degradation occurred on the anode surface where the pH is controlled more by the anodic reactions rather than the bulk solution.

A set of experiments were also performed to evaluate the electrooxidation of PFOS with TSO in solutions containing different supporting electrolytes, including 10-mM, 25-mM and 100-mM Na_2SO_4, 100-mM $NaNO_3$ and 100-mM $NaClO_4$. The k_{SA} of L-PFOS degradation obtained in different electrolytes were summarized in Table 3. At the same current density, anodic potential was usually higher in lower concentration electrolyte as seen in Table 3. Therefore, k_{SA} values decreased with increasing electrolyte concentration. The k_{SA} did not vary much for the three different electrolyte solutions at 100-mM.

Taken together, the change in electrolyte type, concentration and pH of the reaction solution appeared to have minimal if any impact on PFOS degradation by electrooxidation on TSO anodes. This may indicate that the bulk solution conditions have very little effect on the anode surface conditions that are mainly controlled by the water oxidation reactions on the anode at our experiment conditions. This may be one advantage in applications to waters of varying conditions. It should be noted though that the conditions having been tested here may differ from those of many PFAS-contaminated wastewaters that have lower electrolyte concentrations and high concentrations of co-existing contaminants. More experiments are needed to draw more conclusive guidelines regarding applications.

3.3 Mixture of PFAAs

Experiments were conducted to evaluate the performance of electrooxidation with TSO anode in a solution containing a mixture of PFAAs including PFBA, PFPeA, PFHxA, PFHpA, PFOA, PFBS, PFHxS and PFOS at varying current densities. Figure 2 displays the concentration profile of each PFAA in the mixture solution during electrooxidation at the current density of 5 mA·cm^{-2} (Figure 2A) and 15 mA·cm^{-2} (Figure 2B) as examples to show the behaviors. Degradation of all 8 PFAAs were evident, with the rates greater at the higher current density, while the degradation rates of PFAAs follow roughly the similar

general order for both high and low current densities: L-PFOS > PFOA > L-PFHxS > PFHpA > PFHxA > L-PFBS > PFPeA > PFBA. Over 90% PFOA and PFOS were removed within 30 minutes at 5 mA·cm^{-2} [22] and within 10 minutes at 15 mA·cm^{-2}. At 15 mA·cm^{-2}, all PFAAs were degraded over 90% except PFBA, which degraded about 50% after 8 hours of electrooxidation treatment. The concentration of fluoride in the solution was also quantified at the end of treatment, and a defluorination ratio was calculated via dividing the released F^- concentration by the total fluorine in the PFAA that has been removed from the system (Text S3). The results are listed in Table S3, and the defluorination ratio were above 90% when the current density was above 10 mA·cm^{-2}.

The surface area normalized pseudo-first order rate constants for PFAA degradation obtained from the electrooxidation treatment of the PFAA mixture at 5 mA·cm^{-2} are also listed in Table 1 to compare with those obtained from the experiment with each PFAA tested individually at the same initial concentration (2.0 μM). It appears that the k_{SA} values in the solutions with PFAA spiked individually are not significantly different from those in the mixture, suggesting minimal competition effect, if any, among PFAAs at the tested concentrations (2.0 μM). The competition effect may however become evident as the concentrations of PFAAs are higher, such as at the levels tested in our previous studies (0.5 mM)[25]. Notably, although the relative order in PFAA degradation rate constants remain the same between solutions with PFAAs spiked individually and in mixture, the k_{SA} values of certain PFAAs increases in the mixture than in the individual solution (e.g. PFOS) while others decreases (e.g. PFOA). Such variation may be attributable to interference or interactions between species during EO reactions, which warrants further investigation.

The degradation of PFAA was evaluated with all PFAAs spiked in mixture under different current densities, and the obtained k_{SA} values are plotted in Figure 3 in relation to the chain lengths and the head functional groups. For each PFAA, the k_{SA} increased with increasing current density. For the PFAAs having the same functional group (PFSAs vs. PFCAs), the increase in carbon chain length led to greater reactivity. This is in accord with other studies showing shorter chain PFAAs more recalcitrant to electrooxidation [17, 31]. For the PFAAs of the same carbon chain length, the ones with sulfonate head group tend to degrade faster than those with carboxylic group.

Increased PFAA removal under higher current densities may be ascribed to the higher anodic potentials as the current density increases before reaching mass transfer rate. Limiting current method was used to measure mass transfer rate of each PFAA on the TSO anode (SI Text S4). Mass transfer rates of all PFAAs are summarized in Table S5. Comparing the data in Table 3 and Table S5 indicates that all PFAA degradation was controlled by EO process in the experimental condition. The surface area normalized degradation rate constant for each PFAA obtained from the experiments with mixture solutions are plotted against anodic potential in Figure 4. It is again evident that the PFAAs with relatively longer carbon chains tend to have greater degradation rates across the tested anodic potential range than the shorter ones, as well as the PFSAs have higher rates than the PFCAs (Figure 4). Regardless of the length of carbon chains, all PFAA degradation rates increased along with the anodic potential. The PFAAs started to exhibit degradation behavior when the anodic potential was above about 2.83 V vs. SHE (standard hydrogen electrode). It is where water oxidation occurs according to linear sweep voltammetry (LSV) shown in Figure S6, which corroborates that the hydroxyl free radicals generated via water oxidation play an essential role in PFAA degradation during electrooxidation on TSO anode [26]. It is regarded that direct electron transfer (DET) and hydroxyl radical attack take place in a concerted manner that lead to PFAA degradation during electrochemical oxidation[17, 32].

3.5. Influence of molecualr structures

In an effort to explain the trends in different degredation rates across tested PFAAs found in this study, the relationships were explored between certain molecular descriptors and the surface area normalized rate constant of PFAA degradation measured in the experiments with solutions each containing an individual PFAA at the current density of 5 $mA \cdot cm^{-2}$. It has been propsoed that the combination of direct electron transfer and hydroxal radical attack plays a major role in the electrooxidative degradtion of PFAA [26]. Therefore, certain molecular and electrical distribution properties of the PFAAs relating to their reactivity with hydroxal radicals and electron transfer have been examined.

Frontier molecular orbital energies often play an important role in determining reactivity of organic chemicals [33]. Energy of the highest occupied molecular orbital (E_{homo}) and the lowest unoccupied molecular orbital (E_{lumo}) represents the ability of a molecule to donate or gain an electron respectively, and the gap between them imply the stability of the molecule in terms of redox reactivity [34 35]. In this study, greater E_{LUMO}-E_{HOMO} gaps were seen for shorter chained PFAAs ranging from 0.244 hartrees for PFBA to 0.155 hartrees for PFOA. It thus makes sense that we have seen a negative correlation between the E_{LUMO}-E_{HOMO} gap and the log k_{sA} (Figure 5A). Indeed, these values form a cohesive negative linear trend through each of the functional groups (PFSAs vs. PFCAs) when plotted log k_{sA} against the E_{LUMO}-E_{HOMO} gap. The energy gap however does not capture the rate constant trend between the functional groups, although this is not surprising given the large difference functional groups make on molecular properties.

Another molecular descriptor of interest, molecular polarizability, indicates the electronic flexibility of each moleucle, thus in connection to the tendency of oxidative reactivity as well as direct electron transfer on anode [36 34]. When plotted against the experimental degredation rate constants found in this study, the molecular polarizability has a nice positive correlation across both functional groups, serving as a good indicator for the reactivety of PFAAs. This suggests that direct electron transfer may be the rate-limiting step in PFAA degradation in TSO-based electooxidation systems, although the hydroxyl radicals generated via water oxidation may also play an role in concert[26].

4. Conclusions

Novel TSO anodes have been shown effective at removing a range of PFCAs and PFSAs in solutions of varying compositions and under a range of operation conditions in this study. The change in electrolyte type, concentration and pH of the reaction solution appeared to have minimal if any impact on PFAA degradation. This is probably because the bulk solution conditions have very little effect on the anode surface conditions that are controlled by the water oxidation reactions on the anode at our experiment conditions. The k_{SA} for PFAA in the mixture was not much different from that obtained when each PFAA was spiked in the solution individually, indicating the absence of strong competitive effect among the PFAA in the mixture under the experiment conditions. For the PFAAs having the same head acid group (PFSAs vs. PFCAs), the increase in carbon chain length led to greater reactivity. For the PFAAs of the same carbon chain length, the ones with sulfonate head group tend to degrade faster than those with carboxylic group. The PFAAs started to exhibit degradation behavior when the anodic potential was above about 2.83 V vs SHE where water oxidation occurs, suggesting that the hydroxyl free radicals generated via water oxidation play a role in PFAA degradation [26]. PFAA degradation rates increased along with the anodic potential. Molecular polarizability, a molecular descriptor of electron flexibility and transfer tendency, appears to be a good indicator for PFAA degradation, suggesting that direct electron transfer may be the rate-limiting step for PFAA degradation in TSO-based electrooxidation systems. Our research indicates the effectiveness of TSO-based electrooxidation and provide a basis for further studies leading to process design and optimization for remediation of PFAS contaminated waters. It should be noted that the experiments performed in this study were with selected PFAAs in simple electrolyte

solutions. More studies are warranted to examine a wider range of PFAS compounds in solutions reflecting actual conditions of PFAS-contaminated water/wastewaters.

Acknowledgements

The study was supported in part by U.S. Department of Defense SERDP ER-2717 and ER-1320. Dr. Shangtao Liang, Dr. Lei Li and Ms. Lu Wang are acklowedged for their helpful dsicussion. Dr. Sayed Hassan is thanked for help with floride analysis.

References

1. S. Fujii, C. Polprasert, S. Tanaka, N. P. Hong Lien and Y. Qiu, New POPs in the water environment: distribution, bioaccumulation and treatment of perfluorinated compounds – a review paper, *Journal of Water Supply: Research and Technology - Aqua*, 2007, **56**, 313-326.
2. J. P. Giesy and K. Kannan, Global Distribution of Perfluorooctane Sulfonate in Wildlife, *Environmental Science & Technology*, 2001, **35**, 1339-1342.
3. I. Ross, J. McDonough, J. Miles, P. Storch, P. T. Kochunarayanan, E. Kalve, J. Hurst, S. S. Dasgupta and J. Burdick, A review of emerging technologies for remediation of PFASs, *Remediation*, 2018, **28**, 101-126.
4. S. Mejia-Avendano, S. V. Duy, S. Sauve and J. X. Liu, Generation of Perfluoroalkyl Acids from Aerobic Biotransformation of Quaternary Ammonium Polyfluoroalkyl Surfactants, *Environmental Science & Technology*, 2016, **50**, 9923-9932.
5. C. Lau, K. Anitole, C. Hodes, D. Lai, A. Pfahles-Hutchens and J. Seed, Perfluoroalkyl acids: a review of monitoring and toxicological findings, *Toxicological sciences : an official journal of the Society of Toxicology*, 2007, **99**, 366-394.
6. C. M. Butt, U. Berger, R. Bossi and G. T. Tomy, Levels and trends of poly- and perfluorinated compounds in the arctic environment, *Sci. Total Environ.*, 2010, **408**, 2936-2965.
7. X. Wang, C. Halsall, G. Codling, Z. Xie, B. Xu, Z. Zhao, Y. Xue, R. Ebinghaus and K. Jones, Accumulation of perfluoroalkyl compounds in tibetan mountain snow: temporal patterns from 1980 to 2010, *Environmental Science and Technology*, 2014, **48**, 173-181.
8. G. W. Olsen, D. C. Mair, C. C. Lange, L. M. Harrington, T. R. Church, C. L. Goldberg, R. M. Herron, H. Hanna, J. B. Nobiletti, J. A. Rios, W. K. Reagen and C. A. Ley, Per- and polyfluoroalkyl substances (PFAS) in American Red Cross adult blood donors, 2000-2015, *Environ. Res.*, 2017, **157**, 87-95.
9. M. F. Rahman, S. Peldszus and W. B. Anderson, Behaviour and fate of perfluoroalkyl and polyfluoroalkyl substances (PFASs) in drinking water treatment: A review, *Water Res.*, 2014, **50**, 318-340.
10. Y. R. Gu, T. Z. Liu, H. J. Wang, H. L. Han and W. Y. Dong, Hydrated electron based decomposition of perfluorooctane sulfonate (PFOS) in the VUV/sulfite system, *Sci. Total Environ.*, 2017, **607**, 541-548.
11. L. Jin and P. Y. Zhang, Photochemical decomposition of perfluorooctane sulfonate (PFOS) in an anoxic alkaline solution by 185 nm vacuum ultraviolet, *Chem. Eng. J.*, 2015, **280**, 241-247.
12. L. Jin, P. Y. Zhang, T. Shao and S. L. Zhao, Ferric ion mediated photodecomposition of aqueous perfluorooctane sulfonate (PFOS) under UV irradiation and its mechanism, *Journal of Hazardous Materials*, 2014, **271**, 9-15.
13. J. Cheng, C. D. Vecitis, H. Park, B. T. Mader and M. R. Hoffmann, Sonochemical Degradation of Perfluorooctane Sulfonate (PFOS) and Perfluorooctanoate (PFOA) in Groundwater: Kinetic Effects of Matrix Inorganics, *Environmental Science & Technology*, 2010, **44**, 445-450.
14. S. Park, L. S. Lee, V. F. Medina, A. Zull and S. Waisner, Heat-activated persulfate oxidation of PFOA, 6:2 fluorotelomer sulfonate, and PFOS under conditions suitable for in-situ groundwater remediation, *Chemosphere*, 2016, **145**, 376-383.
15. K. E. Carter and J. Farrell, Oxidative destruction of perfluorooctane sulfonate using boron-doped diamond film electrodes, *Environmental Science & Technology*, 2008, **42**, 6111-6115.
16. H. Lin, J. F. Niu, S. Y. Ding and L. L. Zhang, Electrochemical degradation of perfluorooctanoic acid (PFOA) by Ti/SnO2-Sb, Ti/SnO2-Sb/PbO2 and Ti/SnO2-Sb/MnO2 anodes, *Water Research*, 2012, **46**, 2281-2289.

17. Q. F. Zhuo, S. B. Deng, B. Yang, J. Huang, B. Wang, T. T. Zhang and G. Yu, Degradation of perfluorinated compounds on a boron-doped diamond electrode, *Electrochimica Acta*, 2012, **77**, 17-22.
18. Q. C. Ma, L. Liu, W. Cui, R. F. Li, T. T. Song and Z. J. Cui, Electrochemical degradation of perfluorooctanoic acid (PFOA) by Yb-doped Ti/SnO2-Sb/PbO2 anodes and determination of the optimal conditions, *RSC Adv.*, 2015, **5**, 84856-84864.
19. B. G. Ruiz, S. Gomez-Lavin, N. Diban, V. Boiteux, A. Colin, X. Dauchy and A. Urtiaga, Efficient electrochemical degradation of poly- and perfluoroalkyl substances (PFASs) from the effluents of an industrial wastewater treatment plant, *Chem. Eng. J.*, 2017, **322**, 196-204.
20. J. Radjenovic and D. L. Sedlak, Challenges and Opportunities for Electrochemical Processes as Next-Generation Technologies for the Treatment of Contaminated Water, *Environmental Science & Technology*, 2015, **49**, 11292-11302.
21. F. C. Walsh and R. G. A. Wills, The continuing development of Magneli phase titanium sub-oxides and Ebonex (R) electrodes, *Electrochimica Acta*, 2010, **55**, 6342-6351.
22. A. M. Zaky and B. P. Chaplin, Mechanism of p-Substituted Phenol Oxidation at a Ti4O7 Reactive Electrochemical Membrane, *Environmental Science & Technology*, 2014, **48**, 5857-5867.
23. P. Geng, J. Y. Su, C. Miles, C. Comninellis and G. H. Chen, Highly-Ordered Magneli Ti4O7 Nanotube Arrays as Effective Anodic Material for Electro-oxidation, *Electrochimica Acta*, 2015, **153**, 316-324.
24. S. T. Liang, H. Lin, X. F. Yan and Q. G. Huang, Electro-oxidation of tetracycline by a Magneli phase Ti4O7 porous anode: Kinetics, products, and toxicity, *Chem. Eng. J.*, 2018, **332**, 628-636.
25. S. T. Liang, R. Pierce, H. Lin, S. Y. Chiang and Q. Huang, Electrochemical oxidation of PFOA and PFOS in concentrated waste streams, *Remediation*, 2018, **28**, 127-134.
26. H. Lin, J. F. Niu, S. T. Liang, C. Wang, Y. J. Wang, F. Y. Jin, Q. Luo and Q. G. Huang, Development of macroporous Magneli phase Ti4O7 ceramic materials: As an efficient anode for mineralization of poly- and perfluoroalkyl substances, *Chem. Eng. J.*, 2018, **354**, 1058-1067.
27. T. X. H. Le, H. Haflich, A. D. Shah and B. P. Chaplin, Energy-Efficient Electrochemical Oxidation of Perfluoroalkyl Substances Using a Ti4O7 Reactive Electrochemical Membrane Anode, *Environmental Science & Technology Letters*, 2019, **6**, 504-510.
28. S. Liang, R. D. Pierce, H. Lin, S.-Y. Chiang and Q. Huang, Electrochemical oxidation of PFOA and PFOS in concentrated waste streams, *Remediation Journal*, 2018, **28**, 127-134.
29. D. A. Skoog, F. J. Holler and T. A. Nieman, *Principles of instrumental analysis*, Belmont (Calif.) : Brooks/Cole, 5th ed. / edn., 1998.
30. A. Lasia, Porous electrodes in the presence of a concentration gradient, *Journal of Electroanalytical Chemistry*, 1997, **428**, 155-164.
31. C. E. Schaefer, C. Andaya, A. Urtiaga, E. R. McKenzie and C. P. Higgins, Electrochemical treatment of perfluorooctanoic acid (PFOA) and perfluorooctane sulfonic acid (PFOS) in groundwater impacted by aqueous film forming foams (AFFFs), *Journal of Hazardous Materials*, 2015, **295**, 170-175.
32. B. P. Chaplin, Critical review of electrochemical advanced oxidation processes for water treatment applications, *Environmental Science: Processes & Impacts*, 2014, **16**, 1182-1203.
33. Z. W. Cheng, B. W. Yang, Q. C. Chen, W. C. Ji and Z. M. Shen, Characteristics and difference of oxidation and coagulation mechanisms for the removal of organic compounds by quantum parameter analysis, *Chem. Eng. J.*, 2018, **332**, 351-360.
34. H. Kusic, B. Rasulev, D. Leszczynska, J. Leszczynski and N. Koprivanac, Prediction of rate constants for radical degradation of aromatic pollutants in water matrix: A QSAR study, *Chemosphere*, 2009, **75**, 1128-1134.

35. C. G. Zhan, J. A. Nichols and D. A. Dixon, Ionization potential, electron affinity, electronegativity, hardness, and electron excitation energy: Molecular properties from density functional theory orbital energies, *J. Phys. Chem. A*, 2003, **107**, 4184-4195.
36. X. H. Jin, S. Peldszus and P. M. Huck, Predicting the reaction rate constants of micropollutants with hydroxyl radicals in water using QSPR modeling, *Chemosphere*, 2015, **138**, 1-9.

Table 1. Surface area normalized pseudo-first order rate constants (k_{SA}) for each PFAA tested both in experiments with solutions containing each individually or in mixture in 100 mM Na_2SO_4 at 5 mA/cm^2. Error represents standard deviation of duplicate experiments results.

Chemicals	Individual $\boldsymbol{k_{SA}}$ ($m \cdot s^{-1}$)	Mixture $\boldsymbol{k_{SA}}$ ($m \cdot s^{-1}$)	Literature ($m \cdot s^{-1}$)
L-PFOS	$8.81 \times 10^{-6} \pm 1.02 \times 10^{-6}$	$1.11 \times 10^{-5} \pm 3.87 \times 10^{-7}$	4.30×10^{-6} in batch system[26 a] 4.40×10^{-5} in REM system[27 b]
PFOA	$5.74 \times 10^{-6} \pm 5.49 \times 10^{-8}$	$4.09 \times 10^{-6} \pm 4.56 \times 10^{-8}$	1.13×10^{-5} in batch system[26 c] 1.30×10^{-4} in REM system[27 b]
PFHpA	$1.26 \times 10^{-6} \pm 7.04 \times 10^{-9}$	$1.62 \times 10^{-6} \pm 2.04 \times 10^{-8}$	
PFHxS	$2.57 \times 10^{-6} \pm 1.64 \times 10^{-7}$	$2.59 \times 10^{-6} \pm 2.02 \times 10^{-7}$	
PFHxA	$5.02 \times 10^{-7} \pm 5.87 \times 10^{-9}$	$3.42 \times 10^{-7} \pm 4.01 \times 10^{-9}$	
PFPeA	$5.99 \times 10^{-8} \pm 2.45 \times 10^{-9}$	$1.19 \times 10^{-7} \pm 5.12 \times 10^{-9}$	
PFBS	$1.75 \times 10^{-7} \pm 7.88 \times 10^{-9}$	$1.59 \times 10^{-7} \pm 4.44 \times 10^{-9}$	
PFBA	$3.49 \times 10^{-8} \pm 4.17 \times 10^{-9}$	$7.94 \times 10^{-8} \pm 7.76 \times 10^{-9}$	

[a]. The initial concentration of PFOS was 0.1 mM, the electrolyte was 20-mM $NaClO_4$;
[b]. The initial concentration of PFOA/PFOS was 10 μM, the electrolyte was 100-mM K_2HPO_4;
[c]. The initial concentration of PFOA was 0.5 mM, the electrolyte was 20-mM $NaClO_4$.

Table 2. Surface area normalized pseudo-first order rate constant (k_{SA}) for PFOS degradation during electrooxidation in solutions of different pH at 5 mA·cm^{-2}. Error represents standard deviation of duplicate experiments results.

Electrolyte	**pH**	**Anodic potential (V vs. SHE)**	$\boldsymbol{k_{SA}}$ **(m·s^{-1})**
50 mM H_2SO_4	1.95-2.20	2.660	$5.72 \times 10^{-6} \pm 5.46 \times 10^{-7}$
100 mM NaOH	12.40-12.55	2.932	$7.89 \times 10^{-6} \pm 1.94 \times 10^{-7}$
100 mM Phosphate Buffer	7.03-7.29	2.938	$7.89 \times 10^{-6} \pm 6.02 \times 10^{-7}$

Table 3. Surface area normalized pseudo-first order rate constant for L-PFOS degradation during electrooxidation in solutions of different electrolytes at 5 mA·cm^{-2}. Error represents standard deviation of duplicate experiments results.

Electrolyte	**Anodic Potential (V vs. SHE)**	$\boldsymbol{k_{SA}}$ **(m·s^{-1})**
10-mM Na_2SO_4	3.672	$1.30 \times 10^{-5} \pm 2.34 \times 10^{-7}$
25-mM Na_2SO_4	3.379	$1.26 \times 10^{-5} \pm 1.94 \times 10^{-7}$
100-mM Na_2SO_4	3.114	$8.81 \times 10^{-6} \pm 2.42 \times 10^{-7}$
100-mM $NaNO_3$	3.204	$9.26 \times 10^{-6} \pm 4.14 \times 10^{-7}$
100-mM $NaClO_4$	3.313	$9.91 \times 10^{-6} \pm 2.90 \times 10^{-7}$

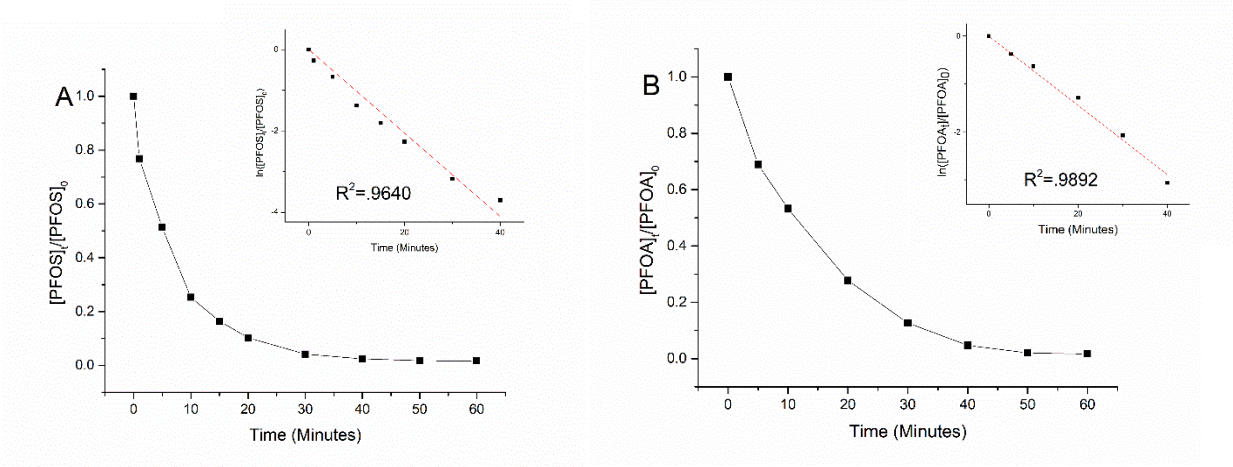

Figure 1. The concentration of PFOS (A) and PFOA (B) over time during electrooxidation with TSO anode at 5.0 mA·cm^{-2}. The test solutions contained each PFAA individually at the Initial concentration of 2.0 μM in 100 mM Na_2SO_4 as supporting electrolyte. Insert shows fit to the pseudo-first rate model.

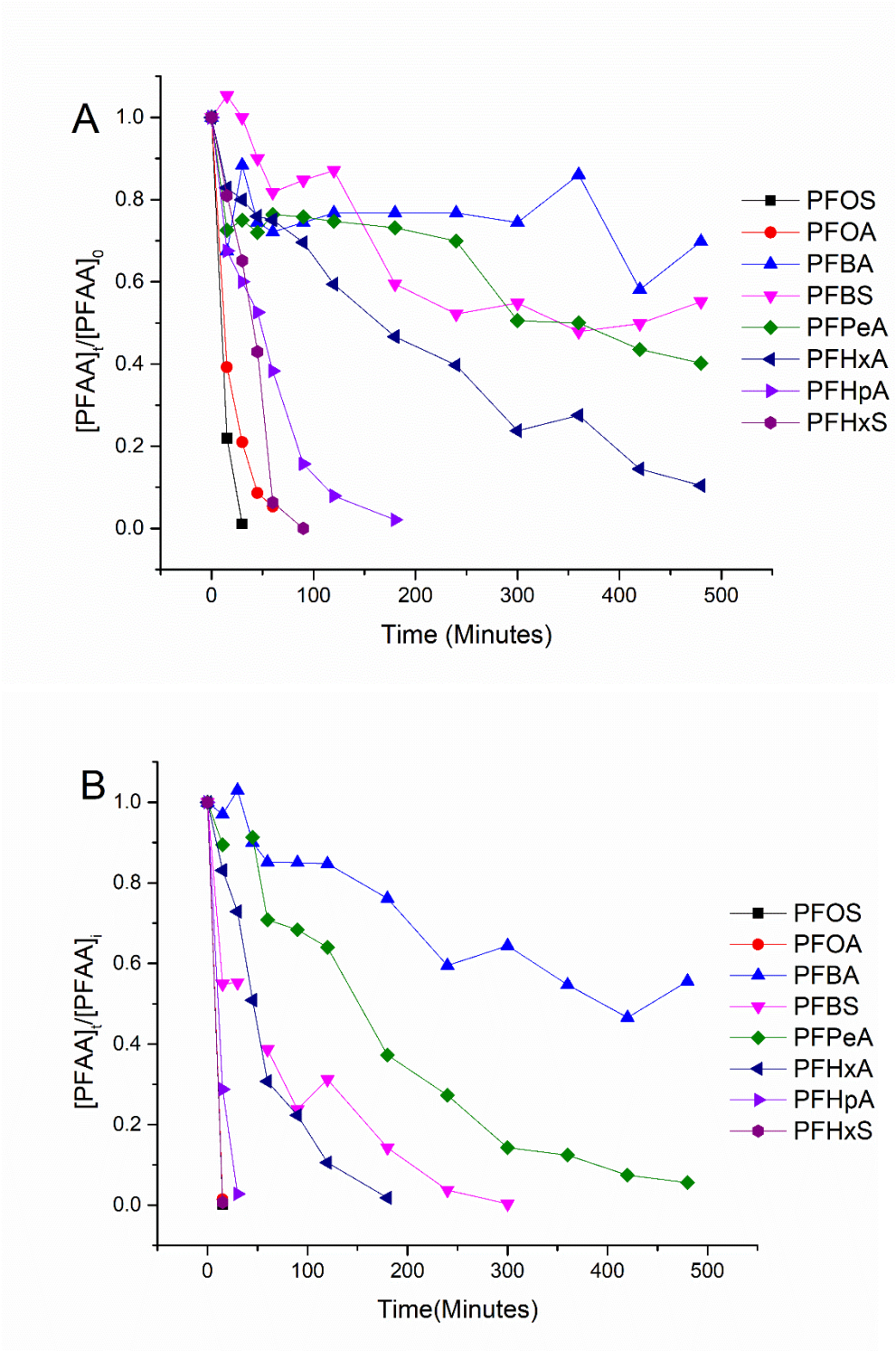

Figure 2. The concentration of each PFAA over time during electrooxidation with TSO anode at 5 mA·cm^{-2} (A) and 15 mA·cm^{-2} (B). The test solutions contained all PFAAs in mixture with each at the initial solution of was 2.0 μM in 100-mM Na_2SO_4 as supporting electrolyte.

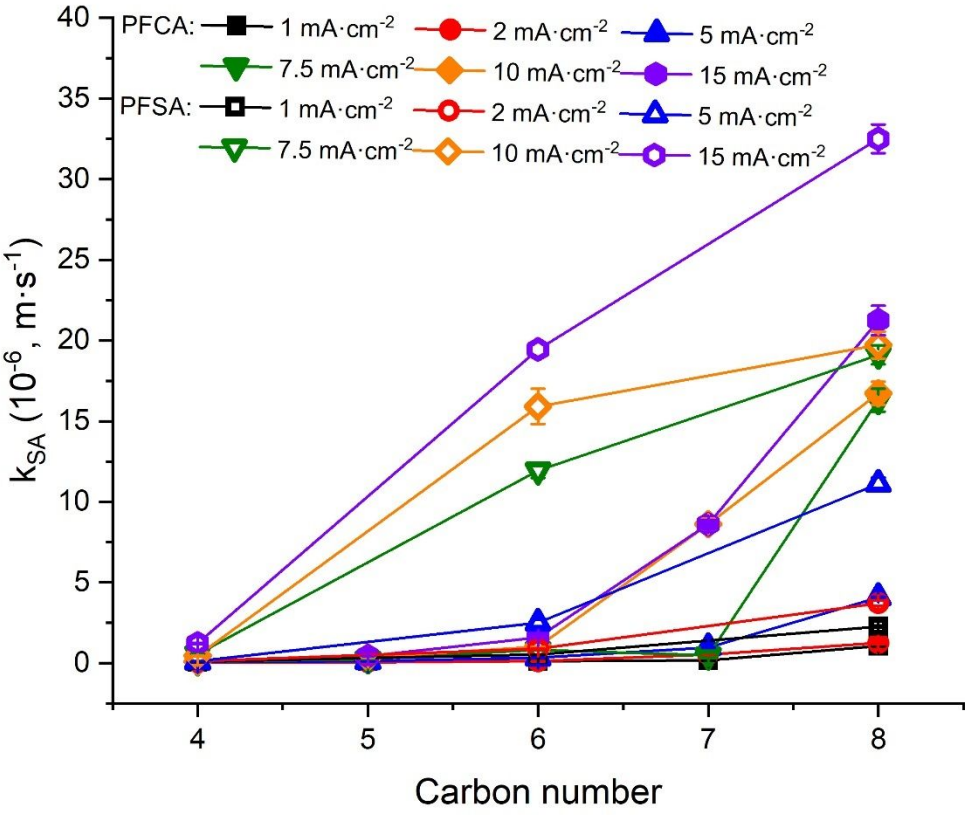

Figure 3. The k_{SA} values of PFAAs of different carbon chain lengths and head functional groups, obtained in electrooxidation experiment with TSO anodes at different current densities. The test solutions contained all PFAAs in mixture with each at the initial solution of was 2.0 μM in 100-mM Na_2SO_4 as supporting electrolyte. Error bar represents standard deviation.

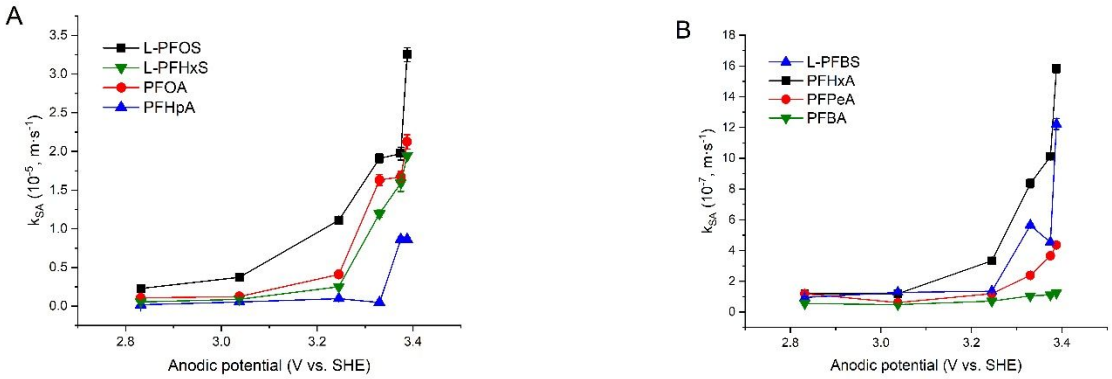

Figure 4. The k_{SA} values of 8 PFAAs plotted against the anodic potential vs. SHE (standard hydrogen electrode) for electrooxidation. The test solutions contained all PFAAs in mixture with each at the initial solution of was 2.0 μM in 100-mM Na_2SO_4 as supporting electrolyte. Error bar represents standard deviation. The data are shown in two figures according to magnitudes for better observation.

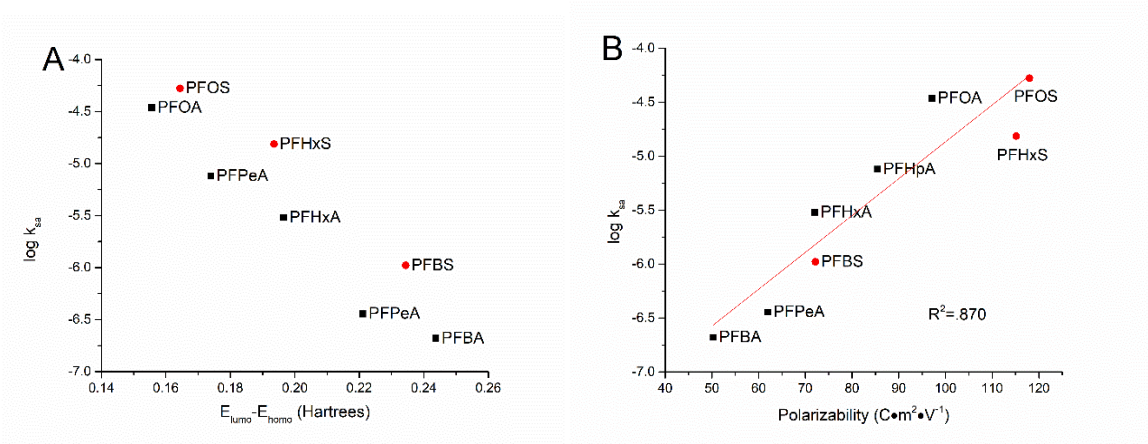

Figure 5. Relationship between the logrithm of the surface area normalized rate constants and E_{LUMO}-E_{HOMO} gap (A) and molecular polarizability (B).

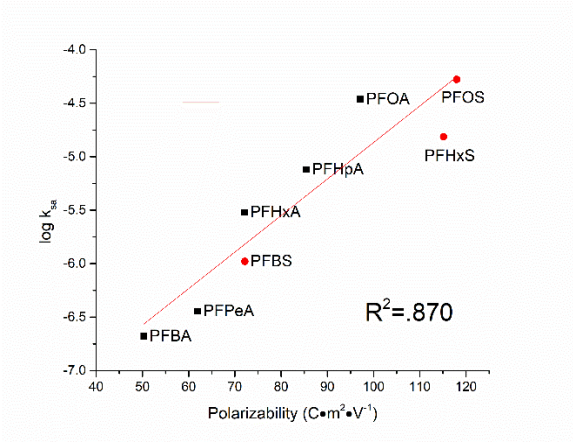

Effective degradation of eight perfluoroalkyl acids by electrooxidation on titanium suboxide anode is correlated to their respective molecular structures, offering insight into their degradation behaviors.